Discovery of a novel analogue of FR901533 and the corresponding biosynthetic gene cluster from *Streptosporangium roseum* No. 79089

Fuchao Xu[1] • Yonghong Liang[1,2] Jie Ren[1] • Siyuan Wang[1] • Jixun Zhan[1]

[1] Department of Biological Engineering, Utah State University, 4105 Old Main Hill, Logan, UT 84322-4105, USA

[2] Key Laboratory of Modern Preparation of TCM, Ministry of Education, Jiangxi University of Traditional Chinese Medicine, Nanchang, Jiangxi 330004, China

Correspondence: Jixun Zhan

jixun.zhan@usu.edu

Abstract

FR901533 (**1**, also known as WS79089B), WS79089A (**2**), and WS79089C (**3**) are polycyclic aromatic natural products with promising inhibitory activity to endothelin-converting enzymes. In this work, we isolated five tridecaketide products from *Streptosporangium roseum* No. 79089, including **1**-**3**, benaphthamycin (**4**) and a novel FR901533 analogue (**5**). The structure of **5** was characterized based on spectroscopic data. Compared to the major product **2**, the new compound **5** has an additional hydroxyl group at C-12 and an extra methyl group at the 13-OH. The configuration of C-19 of these compounds was determined to be *R* using Mosher's method. A putative biosynthetic gene cluster for compounds **1-5** was discovered by analyzing the genome of *S. roseum* No. 79089. This 38.6-kb gene cluster contains 38 open reading frames, including a minimal polyketide synthase (*wsaA*-*C*), an aromatase (*wsaD*), three cyclases (*wsaE*, *F* and *W*) and a series of tailoring enzymes such as monooxygenases (*wsaO1*-*O7*) and methyltransferases (*wsaM1* and *M2*). Disruption of the ketosynthase gene (*wsaA*) in this gene cluster abolished the production of **1**-**5**, confirming that this gene cluster is indeed responsible for the biosynthesis of **1**-**5**. A type II polyketide biosynthetic pathway was proposed for this group of natural endothelin-converting enzyme inhibitors.

Key points

- Five aromatic tridecaketides were isolated from *Streptosporangium roseum* No. 79089.
- A novel FR901533 analogue, 12-hydroxy-13-*O*-methyl-WS79089A, was characterized.
- The absolute configuration of C-19 of FR901533 and analogues was determined.
- The biosynthetic gene cluster of FR901533 and analogues was discovered.

Keywords FR901533・endothelin-converting enzyme inhibitor・polyketide biosynthesis・*Streptosporangium roseum*・gene disruption

Introduction

Endothelin (ET) is a potent vasoconstrictor peptide released from renal endothelial and other cells, which exists in three isoforms, ET-1, ET-2, and ET-3 (Davenport et al. 2016). They are 21-amino acid peptides, with ET-1 being the most abundant isoform. ETs are involved in maintaining the balance between vasoconstriction and vasodilation in the normal human cardiovascular system. However, overexpression of ETs can contribute to high blood pressure, which can hurt heart, general circulation and brain (Coelho et al. 2018), and leads to cancer (Bagnato et al. 2008), pain mediation (Smith et al. 2014), cerebral vasospasm (Cheng et al. 2018) and other cardiovascular disorders.

Physiologically active ETs are formed from big ETs by endothelin-converting enzymes (ECEs) through the selective cleavage at the Trp_{21}-Val/Ile_{22} peptide bond (Johnson et al. 1999). Two major forms of ECE, including ECE-1 and ECE-2, have been reported (Emoto and Yanagisawa 1995; Kaburagi et al. 1999). ECE-1 is the enzyme primarily responsible for the synthesis of active ET-1 (Whyteside et al. 2014). ET-1 plays a critical role in cardiovascular diseases (CVDs) such as hypertension, pulmonary hypertension, atherosclerosis, congestive heart failure, and myocardial infarction (Dhaun and Webb 2019; Rodríguez-Pascual et al. 2011). Under these pathophysiological conditions, circulating ET levels in plasma, urine or cerebrospinal fluid are elevated (Löffler 2000). Therefore, inhibition of the ET system may have significant potential for the development of new CVD therapeutics. Two common approaches are used to inhibit ET, including blockade of the ET receptors and inhibition of ECE-1 (Hitzerd et al. 2020; Miyagawa and Emoto 2014). Studies in animal disease models suggested that ECE-1 inhibitors may be used in the treatment of pulmonary hypertension, cardiac hypertrophy and failure, myocardial infraction, restenosis, and acute renal failure (De Lombaert et al. 2000;

Doggrell 2004).

About a half of approved small-molecule therapeutics are either natural products or directly derived from natural products (Newman and Cragg 2020). FR901533 (**1**, also known as WS79089B), WS79089A (**2**), WS79089C (**3**) and benaphthamycin (**4**) shown in Fig. 1 are dihydrobenzo[α]naphthacenequinone natural products produced by actinomycetes (Ritzau et al. 1997; Tsurumi et al. 1994). **1-3** have shown selective inhibitory activity to ECE, with IC_{50} values of 0.14, 0.73 and 3.42 μM, respectively. Among these compounds, **1** is three times more potent than the well-known ECE inhibitor phosphoramidon (IC_{50} = 0.49 μM). Furthermore, **1-3** have also shown great safety profiles. Acute toxicity studies in mice revealed that their LD_{50} values were higher than 100 mg/kg, and did not have any toxicity until day 14 (Tsurumi et al. 1994). Further studies showed that **1** acts as a competitive inhibitor of ECE, with a K_i value of 8.9×10^{-8} M (Tsurumi et al. 1995). Animal studies revealed that **1** can protect the development of right ventricular overload and reduce the degree of medial thickening of pulmonary arteries in rats (Takahashi et al. 1998). It reduced the conversion of big ET-1 to ET-1 in post-myocardial infarction rats and improved some parameters of cardiac remodeling early post-myocardial infarction (Martin et al. 2000). **1** was reported to decrease the blood pressure in apolipoprotein E (*apoE*)-deficient mice fed with a Western-type fat diet (Martínez-Miguel et al. 2009) and calcitriol-treated rats (Martínez-Miguel et al. 2014). Phenylephrine induces the expression of ET-1 in rat cardiac myocytes and increases the conversion of big ET-1 to ET-1. A study found that **1**, as a specific ECE-1 inhibitor, can inhibit the phenylephrine-stimulated increase in protein synthesis rate by 45% (Kaburagi et al. 1999). **1** also decreased plasma renin activity, as well as the levels of plasma atrial natriuretic peptide, angiotensin II, and aldosterone in beagle dogs (Wada et al. 1999). Another study in dogs revealed that **1** decreased pulmonary capillary wedge pressure and increased cardiac output. This compound prevented the reduction of urine flow rate and urinary sodium excretion in association with an increase in the glomerular filtration

rate and renal plasma flow, and significantly suppressed the elevation of plasma atrial natriuretic peptide and aldosterone levels, which is an established prognostic factor in congestive heart failure. These results indicate that chronic ECE inhibition has potential for the treatment of congestive heart failure, not only on hemodynamics but also in the prevention of fluid retention (Wada et al. 2002). Therefore, this family of compounds represent promising lead compounds for the development of new CVD therapeutics.

In continuation of our effort to search for new natural product for drug discovery, a new analogue (**5**) of FR901533 was isolated from *Streptosporangium roseum* No. 79089, along with the known compounds **1-4**. The C-19 configuration was determined using the Mosher method. A putative biosynthetic gene cluster was discovered from the genome of *S. roseum* No. 79089, and its involvement in the biosynthesis of **1-5** was confirmed through gene disruption.

Fig. 1

Materıals and methods

General equipment

Products were analyzed and purified on an Agilent 1200 HPLC instrument with an Agilent Eclipse XDB-C18 column (5 μm, 250 mm × 4.6 mm). The samples were eluted with acetonitrile-water (5:95 to 100:0, v/v) at a flow rate of 1 mL/min for 30 min and detected at 460 nm. ESI-MS spectra were obtained on an Agilent 6130 single quadrupole LC-MS in the negative mode. 1D and 2D NMR spectra were recorded in deuterated dimethyl sulfoxide (DMSO-d_6) on a JEOL ECX-300 NMR instrument (300 MHz for ^{1}H NMR and 75 MHz for ^{13}C NMR) or a Bruker Avance III HD Ascend-500 NMR instrument (500 MHz for ^{1}H NMR and 125 MHz for ^{13}C NMR) in the Department of Chemistry and Biochemistry, Utah State University. The chemical shift (δ) values are given in parts per million (ppm). The coupling constants (*J* values) are reported in hertz (Hz).

Strains and vectors

S. roseum No. 79089 (NRRL 2505) was obtained from the USDA Agricultural Research Service Culture Collection. *Escherichia coli* XL-1 Blue (Stratagene) and the pJET1.2 cloning vector (Thermo Fisher) were used for routine subcloning. *E. coli* ET12567 (pUZ8002) and pKC1139 vector were used for the gene disruption experiments.

Media and culture conditions

S. roseum No. 79089 and its mutants were maintained on YM (yeast extract-malt extract) agar plates at 28°C. *E. coli* strains were routinely cultured in Luria-Bertani (LB) broth at 37°C. MS (mannitol soya flour), ISP4 (international *Streptomyces* project medium 4), and TSB (tryptic soy broth) media were used in the conjugation experiments. Ampicillin (50 μg/mL) and apramycin (50 μg/mL) were added to the media appropriately for the cloning or conjugation.

Extraction, analysis and purification of compounds

S. roseum No. 79089 and its disruption mutant were grown on YM agar plates (with or without apramycin). The cultures were extracted three times with an equal volume of methanol. The extracts were then dried under reduced pressure and re-dissolved in methanol for LC-MS analysis. To isolate compounds **2-5**, the cultivation of wild type *S. roseum* No. 79089 was scaled up to 1 L. The plates were maintained at 28°C. After 7 days, the culture was extracted with 1 L of methanol three times. The extract was dried under reduced pressure. The compounds (**2**, **3**, **4** and **5**) were purified by HPLC on a C18 reversed phase column, eluted with acetonitrile-water (5:95 to 100:0, v/v) at a flow rate of 1 mL/min over 30 min, yielding 29.8 mg of **2**, 4.3 mg of **3**, 3.5 mg of **4**, and 5.3 mg of **5**.

Preparation of (*S*)-MTPA (2S) and (*R*)-MTPA (2R) esters

1 mg of **2** was transferred into one clean and completely dry NMR tube. Anhydrous pyridine-d_5 (0.4 mL) and *R*-(+)-α-methoxy-α-(trifluoromethyl) phenylacetyl chloride [(*R*)-MTPA-Cl]

were added to the NMR tube quickly, and the NMR tube was shaken carefully to evenly mix the sample with (*R*)-MTPA-Cl. The reaction mixture was allowed to stand at room temperature for 12 hours to yield the corresponding (*S*)-MTPA ester **2S**. Similarly, 1 mg of **2** was reacted with (*S*)-MTPA-Cl to yield the corresponding (*R*)-MTPA ester **2R**. The ^{1}H NMR spectra of **2S** and **2R** were collected on a Bruker Avance III HD Ascend-500 NMR instrument. The Δδ (δ_{2S}−δ_{2R}) values for proton signals near C-19 were calculated.

Analysis of *the* genome of *S. roseum* and annotation of the putative *wsa* biosynthetic gene cluster

The genome of *S. roseum* No. 79089 (GenBank accession number CP001814) has been previously reported (Nolan et al. 2010). Analysis of the sequenced genome was performed with RAST (rapid annotation using subsystem technology) (Overbeek et al. 2013). The *wsa* gene cluster was annotated with FramePlot (Ishikawa and Hotta 1999).

Plasmid construction for the disruption of *wsaA* in *S. roseum* No. 79089

To find out whether the discovered gene cluster is involved in the biosynthesis of **1-5**, a 732-bp fragment of the putative ketosynthase gene *wsaA* was amplified from the genomic DNA of *S. roseum* No. 79089 with a 30-cycle PCR program (15 s at 98°C, 15 s at 62°C, and 30 s at 72°C). The two primers were used, including 2505-KS-KO-F-*Eco*RI (5'-AAGAATTCGTAACATCACGCTGTTCGAC-3') and 2505-KS-KO-R-*Hin*dIII (5'-AAAAGCTTTGAGACCGGTCATGTGGTAG-3'). The PCR product was ligated into the pJET1.2 vector. The ligation product was transferred into *E. coli* XL1-Blue. Correct transformants were selected by ampicillin resistance. Colonies were picked into 5 mL of LB broth with 50 μg/mL ampicillin, which were grown at 37°C overnight. Plasmids were extracted and then digested with *Eco*RI and *Hin*dIII. The correct plasmid was named as pSW129. After sequencing, the *wsaA* fragment was excised from pSW129 and ligated into pKC1139 between *Eco*RI and *Hin*dIII to afford pSW130.

Conjugation and verification of the *wsaA*-disrupted mutant of *S. roseum* No. 79089

The gene disruption plasmid pSW130 was introduced into *E. coli* ET12567 (pUZ8002) through chemical transformation. It was then introduced into *S. roseum* No. 79089 by *E. coli–Streptomyces* conjugation, following the previously reported procedure (Bierman et al. 1992; Shao et al. 2012). The resulting *E. coli* strain (*E. coli* ET12567 (pUZ8002)/pSW130) was used as donor and *S. roseum* No. 79089 was the acceptor. The positive colonies were picked into TSB medium with 50 μg/mL of apramycin after 20 days of culture on MS plates. The colonies were grown in TSB medium at 28°C and 250 rpm for 7 days and 50 μL of the culture was spread on ISP4 plates with 50 μg/mL of apramycin. Colonies showing up at 37°C were considered as the recombination strain, which was further cultured on YM plate with 50 μg/mL apramycin at 28°C for product check. The mutants were confirmed by PCR analysis with a set of pKC1139- and genome-specific primers, including M13-47, RV-M, 2505-KS-check-1 (5'-AGTACGTGGCCGAGCACTA-3') and 2505-KS-check-2 (5'-TGAGCACGGAGTCGATCG-3') using a 30-cycle PCR program (30 s at 98°C, 30 s at 58°C, and 60 s at 72°C).

Results

Detection of five major dihydrobenzo[α]naphthacenequinone compounds in the culture of *S. roseum* NRRL 2505

S. roseum No. 79089 was grown in YM agar and analyzed by LC-MS. As shown in trace i of Fig. 2a, five major products were detected at 460 nm. These compounds had a similar maximum UV absorption at ~460 nm, suggesting that they are structurally related analogues. ESI-MS spectra (Figs. 2b-2f) of **1-5** showed the corresponding quasimolecular ion $[M-H]^-$ at *m/z* 505.2,

487.1, 529.3, 503.0 and 517.2, indicating that the molecular weights of **1**-**5** are 506, 488, 530, 504 and 518, respectively.

These compounds were purified and subjected to NMR analysis. The major product **2** has a molecular weight of 488, which is consistent with that of WS79089A previously isolated from this strain. Its ^{1}H NMR data (Table S1) are in good agreement with those reported (Tsurumi et al. 1994), confirming that compound **2** is WS79089A. Compound **1** has a molecular weight of 504, which is 18 mass units larger than **1**, suggesting that a water molecule has been added into the structure of **2**. This molecular weight is the same as that of FR901533, also named WS79089B, a hydrolyzed derivative of **2**. Indeed, **2** can be easily converted to **1** in the presence of 1 N NaOH (Fig. S1), further supporting that **1** is FR901533. Similarly, the structures of **3** and **4** were characterized as WS79089C and benaphthamycin, respectively, by a comparison of their ^{1}H NMR (Table S1) with literature (Ritzau et al. 1997; Tsurumi et al. 1994).

Fig. 2

Characterization of 5 as 12-hydroxy-13-*O*-methyl-WS79089A

The molecular weight of **5** was determined to be 518, which is 30 mass units larger than the major product **2**. The 1D and 2D NMR of **5** were collected. The ^{13}C NMR spectrum of **5** revealed 28 carbon signals (Table 1), with one additional methoxy signal at δ_C 61.3 than the major product **2**, suggesting that one of the hydroxyl groups has been methylated. This was supported by the OCH_3 signal at δ_H 3.86 in the ^{1}H NMR (Table 1). The NMR data also revealed that one aromatic CH has been hydroxylated, indicated by the absence of an aromatic proton signal and the appearance of a low field aromatic quaternary carbon signal at δ_C 159.0. Overall, the introduction of a hydroxyl group and a methyl group is consistent with the mass difference (30 Da) between **2** and **5**.

Table 1

A further comparison of the ^{1}H NMR data of **5** (Table 1) and **2** (Table S1) indicated that the major difference lies in ring A. The three free aromatic proton signals on ring A of **2** include two overlapped signals at δ_H 7.71-7.88 that belong to H-10 and H-11 and a dd (doublet of doublets) H-12 signal at δ_H 7.38 (Table S1). However, there were only two aromatic proton signals on the same ring of **5**, including a doublet at δ_H 7.93 and a doublet at δ_H 7.28 (Table 1). The coupling constant of these two doublets are 8.6 Hz, indicating that these two protons are *ortho* to each other. The signal at δ_H 7.93 was assigned to H-10 due to its HMBC correlation to C-8 at δ_C 188.0 (Fig. 3). Therefore, the other aromatic proton signal at δ_H 7.28 must belong to H-11. The presence of H-10 and H-11 indicated that C-12 was hydroxylated. Furthermore, the HMBC correlation of the newly introduced methoxy signal at δ_H 3.86 to C-13 at δ_C 147.5 (Fig. 3) confirmed that the 13-OH was methylated. Therefore, **5** was identified as 12-hydroxy-13-*O*-methyl-WS79089A, which is a new compound and was named as WS79089D.

Fig. 3

Determination of the absolute configuration of the C-19 of WS79089A

Compounds **1-5** have a hydroxyl group at C-19. The 19-OH of **1**, **2**, **4** and **5** is free, while that of **3** was acetylated (Fig. 1). To find the configuration of this hydroxyl group, we chose the major product **2** to prepare the Mosher esters. This compound was reacted with *R*- and *S*-MTPA chloride in deuterated pyridine in NMR tubes to afford the corresponding *S*- and R-MTPA ester derivatives, **2S** and **2R**. The ^{1}H NMR of these MTPA esters were collected. The $\Delta\delta$ ($[\delta_S-\delta_R]$) values near C-19 were calculated and are shown in Fig. 4, which revealed that the absolute configuration of C-19 is *R*. This is same as C-19 in pradimicin A, whose configuration was found to be *R* as well (Napan et al. 2014). Therefore, based on our results, the 19-OH of **2** was determined to be in an β configuration.

Fig. 4

Discovery of a putative WS79089 (*wsa*) biosynthetic gene cluster and the proposed biosynthetic pathway

The structures of **1-5** indicated that they are synthesized through a type II polyketide biosynthetic pathway. By searching the reported genomic sequence of *S. roseum* No. 79089 in the NCBI GenBank, a putative type II PKS gene cluster for the biosynthesis of WS79089A (*wsa*) and analogues was located in this strain. As shown in Fig. 5a, this 38.6 kb *wsa* gene cluster contains 38 open reading frames (orfs). Their putative functions were predicted based on BLAST analysis of the corresponding amino acid sequences (Table 2). This gene cluster has 3 regulatory genes (*wsaR1, R2* and *R3*), a minimal PKS (*wsaA*, *B* and *C*), an aromatase (*wsaD*), three cyclases (*wsaE, F* and *W*), three ketoreductases (*wsaG, T* and *V*), two methyltransferases (*wsaM1* and *M2*), and a number of other tailoring enzymes such as monooxygenases (*wsaO1-O6*) and oxidoreductases (*wsaJ* and *wsaH1-H5*). There are also hypothetical proteins (*wsaU1-U3*), asparagine synthetase (*wsaN*), and nitroreductase (*wsaP*) that might not be involved in the biosynthesis of **1**-**5**.

Fig. 5

The *wsa* minimal PKS, including WsaA (ketosynthase), WsaB (chain length factor) and WsaC (acyl carrier protein), is proposed to generate a nascent 26-carbon poly-β-ketone intermediate **6** by condensing acetyl-CoA with 12 units of malonyl-CoA. The ketone group at C-11 is then reduced by a ketoreductase (WsaV or WsaT) to a hydroxyl to yield **7**. The hydroxyl group will be removed when ring A and B are cyclized by the aromatase WsaD, which leads to a free proton at C-11 in the intermediate **8** and the final structure of **1**-**5**. It was reported that in the biosynthesis of pradimicin A, a pentangular aromatic polyketide, the closure of rings C-E requires synergistic actions of two cyclases and a ring B monooxygenase (Zhan et al. 2008). We proposed that a similar approach is also adopted in the biosynthetic pathway of **1**-**5**. WsaE and WsaF will work with WsaO3, a homolog of the pradimicin ring B monooxygenase PdmH,

to yield the pentangular intermediate **9**. A ketoreductase, WsaV or WsaT reduces the 25-ketone to a hydroxyl group to afford **10**. Another ketoreductase, WsaG, will reduce the 19-ketone of **10** to a hydroxyl group to generate **11**. One of the monooxygenases will introduce a hydroxyl group to C-5 to yield **12**. Finally, methylation of the 17-OH of **12** will lead to the formation of **1**. Closure of ring F by the putative cyclase WsaW can convert **1** to the major product **2**. Compounds **3** and **4** can be formed from **2** by acetylation at the 19-OH and hydroxylation at C-24, respectively. **2** can also be hydroxylated at C-12 and methylated at the 13-OH to give rise to **5**. The proposed biosynthetic pathway of **1-5** is shown in Fig. 5b. The order of the tailoring steps is to be determined.

Table 2

Confirmation of the involvement of the *wsa* gene cluster in WA79089 biosynthesis

To find out whether this type II polyketide biosynthetic gene cluster is involved in the biosynthesis of **1** and its analogues, we conducted a gene disruption experiment. The ketosynthase catalyzes the decarboxylative condensation of the starter unit (acetyl-CoA) with the extender unit (malonyl-CoA), and thus plays an essential role in the biosynthetic process. We cloned a 732-bp gene fragment from the putative ketosynthase gene *wsaA* into pKC1139, yielding the disruption plasmid pSW130 (Fig. 6a). This plasmid was transferred into *S. roseum* No. 79089 through *E. coli* ET12567-mediated conjugation. After integration of the plasmid integrated into the genome, the recombination mutant was selected by apramycin resistance and regrown in YM with apramycin for extraction of the genomic DNA. The disruption of *wsaA* was verified by PCR. When primers 1 and 2 were used, a 1.5-kb fragment was amplified from the wild type, but was not obtained from the mutant due to the insertion of a large plasmid (pSW130) into the genome (Fig. 6b). When primers 1 and M13-47 were used, a 1.1-kb PCR product was obtained. This fragment could not be amplified from the wild type due to the use of the vector-specific primer M13-47 (Fig. 6b). Similarly, when primers 2 and RV-M were used,

the expected 1.09-kb fragment was amplified from the mutant, but not the wild type (Fig. 6b). All these results confirmed that the *wsaA* gene of *S. roseum* No. 79089 was successfully disrupted. The correct *wsa*A-disrupted mutant was grown in YM supplemented with apramycin and the extract was analyzed by HPLC. As shown in trace ii of Fig. 2a, the production of **1-5** was abolished in this mutant, confirming that WsaA is essential for the production of these compounds in *S. roseum* No. 79089. Therefore, the *wsa* gene cluster was confirmed to be truly responsible for the biosynthesis of **1-5**.

Fig. 6

Discussion

Natural products are a rich source of bioactive molecules, such as penicillin (antimicrobial), tetracycline (antimicrobial), paclitaxel (anticancer) and lovastatin (anticholesterol). Polyketides are a group of structurally and functionally diverse natural products, including **1-5** studied in this work. The main polyketide chain for these polycyclic aromatic compounds contains 26 carbons, and thus are among the longest polyketide natural products that have been discovered in nature. Several known long aromatic polyketides have been previously reported to possess interesting biological activities, such as pradimicins (antifungal and antiviral) (Nakagawa et al. 2013), benastatins (antibacterial and glutathione *S*-transferase inhibitory) (Jiang et al. 2020), and fredericamycins (antitumor) (Kotha et al. 2019).

1-5 belong to the group of tridecaketides. Few tridecaketides have been previously reported. For example, accramycin A is an aromatic tridecaketide natural product isolated from *Streptomyces* sp. MA37. This compound showed antibacterial activity against Group B *Streptococcus*, with a minimum inhibitory concentration (MIC) of 27 μg/mL (Maglangit et al. 2019). In addition to aromatic tridecaketides, linear polyene tridecaketides have also been reported. For instance, mycenaaurin A is a pigment from *Mycena aurantiomarginata*, which

consists of a tridecaketide backbone connected with two amino acid moieties. It also showed antibacterial activity against *Bacillus pumilus* (Jaeger and Spiteller 2010). **1-3** are specific inhibitors of ECE. **2** is identical to **1** except that its ring F is closed. It can be easily converted to **1** under alkaline conditions (Fig. S1). **4** was co-isolated with **2** from *Streptomyces* sp. HKI-0057. It showed moderate antibacterial activity against Gram-positive bacteria such as *Bacillus subtilis*. This compound also displayed cytopathic effect against animal cells such as K-562 human leukemia cells (Ritzau et al. 1997). **4** is the 24-hydroxylated derivative of **2**. This is the first time this compound was isolated from *S. roseum* No. 79089. Furthermore, **5** was isolated from *S. roseum* No. 79089 and structurally characterized as a new member of the WS79089A family. This new compound is also an analogue of **2**, with structural variations at C-12 and C-13. Specifically, it is derived from **2** by the 12-hydroxylation and 13-O-methylation, attributing to the diverse tailoring enzymes in the *wsa* gene cluster. Isolation of **5** from *S. roseum* No. 79089 provides a new compound for testing of the ECE inhibitory activity.

1-5 contain a hydroxyl group at C-19. The configuration of C-19 of the major metabolite **2** was determined to be *R* using the Mosher method, indicating that there is a β hydroxyl group at this position. Because of the same biosynthetic origin, it is believed that this is also the case for **1** and **3-5**. The configuration of C-19 in **1-5** is same as that reported for hexaricin A, which was determined to be *R* based on circular dichroism spectrum (Tian et al. 2016). Pradimicins also have a hydroxyl group at this position. We have previously determined the configuration of C-19 of pradimicins using a similar method (Napan et al. 2014). It was found that this carbon also has a *R* configuration, meaning that the 19-OH in pradimicins is in a β configuration. This hydroxyl group was introduced by a dedicated cytochrome P450 (CYP) hydroxylase (Napan et al. 2014). However, there are no putative CYP enzymes in this gene cluster (Table 2). Instead, we propose that the 19-OH is formed through the reduction of the 19-ketone group by a dedicated ketoreductase. PdmG was previously found to catalyze the reduction of the 19-ketone

to a hydroxyl group. This 19-OH is likely to be removed by dehydration to yield a double bond, which is then reduced to afford a single bond between C-19 and C-20, as seen in the pradimicin biosynthetic intermediate G-2A (Zhan et al. 2008). BLAST analysis revealed that WsaG is homologous to PdmG, with 56% identity and 74% similarity. Therefore, it is reasonable to propose that WsaG is the enzyme responsible for reducing the ketone group to hydroxyl at C-19.

The *wsa* gene cluster is highly similar to that reported for hexaricins in *Streptosporangium* sp. CGMCC 4.7309 (Tian et al. 2016). The involvement of this gene cluster in the biosynthesis of **1**-**5** was confirmed through targeted disruption of the *wsaA* gene (Fig. 6), which encodes a ketosynthase. There are three putative transcriptional regulatory genes in the *wsa* gene cluster, including *wsaR1*, *R2* and *R3*. While *wsaR2* sits inside the gene cluster, *wsaR1* and *wsaR3* are at the two ends. The sequence of *wsaR1* is similar to *acnR*, a tet regulatory gene found in the actinomycin D biosynthetic pathway from marine-derived *Streptomyces costaricanus* SCSIO ZS0073 (Liu et al. 2019). Based on the sequence homology, the other two regulatory genes are proposed to be a TenA family transcriptional regulator and SARP family transcriptional regulator, respectively. These two regulatory genes correspond to Hex17 and Hex1 reported in the *hex* gene cluster. Manipulation of regulatory genes in natural product biosynthetic pathways is a useful approach to enhance the yields of selected products (Fidan et al. 2019; Lu et al. 2017; Sun et al. 2018). Therefore, they are interesting targets to identify and engineer. The minimal PKS, consisting of *wsaA*, *wsaB* and *wsaC*, are homologous to PdmA, B and C in pradimicin biosynthesis, with 70%-86% similarities (Table 2). PdmA, B and C were previously characterized as the minimal PKS for pradimicin biosynthesis through heterologous expression. These three enzymes generate a 24-carbon poly-β-ketone chain (Zhan et al. 2008). WsaA, B and C are expected to create a nascent tridecaketide chain that contains 26 carbons. While we have not expressed these enzymes in a heterologous host, a gene disruption was

conducted for *wsaA*. Our results showed that disruption of *wsaA* abolished the production of **1-5**, indicating that this enzyme is essential for the assembly of the core tridecaketide structure.

The nascent poly-β-ketone chain is highly reactive and is supposed to be cyclized by associated aromatase and cyclases immediately. However, unlike pradimicins and benastatins, the structures of **1-5** lack the 11-OH. This suggested that the 26-carbon poly-β-ketone intermediate is reduced at C-11. There are three putative ketoreductase genes in the *wsa* gene cluster, including *wsaG*, *wsaV* and *wsaT*. One of these ketoreductases is supposed to catalyze the reduction. The corresponding hydroxyl group at C-11 will be eliminated by dehydration during the cyclization and aromatization of ring A. The pradimicin biosynthetic gene cluster contains an aromatase (PdmD) and two cyclases (PdmK and PdmL). PdmD closes rings A and B of pradimicin A, and PdmK and PdmL are involved in the closure of rings C-E. In this work, we found that the *wsa* biosynthetic gene cluster also contains the corresponding genes, including the putative aromatase gene *wsaD* and cyclase genes *wsaE* and *wsaF*. However, there is an additional cyclase gene, *wsaW*, in this gene cluster. We propose that this gene might be involved in the closure of ring F of **2-5**.

Monooxygenases are commonly found in aromatic polyketide biosynthesis and contribute to the structural diversity of natural products. They can catalyze a series of reactions such as hydroxylation and oxidation. Monooxygenases have been reported to have a role in fidelity control during aromatic polyketide biosynthesis (Qin et al. 2019). In addition, these enzymes are known to work with other tailoring enzymes such as cyclases synergistically. For instance, PdmH is the ring B monooxygenase to form the quinone structure in pradimicins. This enzyme works with two cyclases, PdmK and PdmL, to close rings C-E to form the core pentangular structure of pradimicins (Zhan et al. 2008). While **2-5** have six rings, we propose that **1** is their precursor with a pentangular structure. There is a putative monooxygenase, WsaO3, in the *wsa* gene cluster. Its amino acid sequence shares 58% identity and 73% similarity

with that of PdmH. Therefore, it was proposed to have a similar function and be responsible for ring B quinone formation by working with two cyclases to form the pentangular structure of **1**. There are six additional monooxygenases in this gene cluster. Some of them are proposed to catalyze the hydroxylation reactions such at C-6 and C-12. Methyltransferases are also common modifying enzymes in natural product biosynthetic pathways. These enzymes introduce methyl groups to various atoms such as C, O, S and N. Correspondingly, there are different methyl transferases such as C-methyltransferases, O-methyltransferases, S-methyltransferases and N-methyltransferases (Pavkov-Keller et al. 2017). There are two putative O-methyltransferase genes (*wsaM1* and *wsaM2*) in the *wsa* biosynthetic gene cluster. The structure of **1**-**4** contains a OCH_3 group at C-17, while the new compound **5** has an additional methoxy group at C-13. Therefore, WsaM1 and WsaM2 are believed to introduce the two methyl groups to the 17-OH and 13-OH, respectively.

The *wsa* gene cluster in Table 2 contains 38 open reading frames and it is likely some of these genes just sit in the gene cluster but are not involved in the biosynthesis of **1**-**5**. It is also possible that the formation of certain minor compounds, such as **3**, the acetylated derivative of **2**, requires the action of an enzyme not within this gene cluster. In summary, this study discovered a new tridecaketide natural product, determined the configuration of C-19 of **1**-**5**, and reported the gene cluster responsible for the assembly of this group of natural products. Therefore, this work provides valuable information for further understanding and engineering of this biosynthetic pathway to generate new compounds for screening of novel ECE inhibitors.

Author contributions FX and JZ conceived and designed research. FX, YL, JR and SW conducted experiments. FX, YL, JR, SW and JZ analyzed data. FX and JZ wrote the manuscript. All authors read and approved the manuscript.

Funding information The Bruker Avance III HD Ascend-500 NMR instrument used in this research was funded by the National Science Foundation Award CHE–1429195.

Compliance with ethical standards

Conflict of interest The authors declare that they have no conflict of interest.

Ethical approval This article does not contain any studies with human participants or animals performed by any of the authors.

References

Bagnato A, Spinella F, Rosano L (2008) The endothelin axis in cancer: the promise and the challenges of molecularly targeted therapy. Can J Physiol Pharmacol 86(8):473–484. https://doi.org/10.1139/Y08-058

Bierman M, Logan R, O'Brien K, Seno ET, Nagaraja Rao R, Schoner BE (1992) Plasmid cloning vectors for the conjugal transfer of DNA from *Escherichia coli* to *Streptomyces* spp. Gene 116(1):43–49. https://doi.org/10.1016/0378-1119(92)90627-2

Cheng Y, Li W, Dou X, Jia R, Yang H, Liu X, Xu C, Liu J, Cao Y, Luo G (2018) Role of endothelin-1 and its receptors in cerebral vasospasm following subarachnoid hemorrhage. Mol Med Rep 18(6):5229–5236. https://doi.org/10.3892/mmr.2018.9513

Coelho SC, Berillo O, Caillon A, Ouerd S, Fraulob-Aquino JC, Barhoumi T, Offermanns S, Paradis P, Schiffrin EL (2018) Three-month endothelial human endothelin-1 overexpression causes blood pressure elevation and vascular and kidney injury. Hypertension 71(1):208–216. https://doi.org/10.1161/hypertensionaha.117.09925

Davenport AP, Hyndman KA, Dhaun N, Southan C, Kohan DE, Pollock JS, Pollock DM, Webb DJ, Maguire JJ (2016) Endothelin. Pharmacol Rev 68(2):357–418. https://doi.org/10.1124/pr.115.011833

De Lombaert S, Blanchard L, Stamford LB, Tan J, Wallace EM, Satoh Y, Fitt J, Hoyer D, Simonsbergen D, Moliterni J, Marcopoulos N, Savage P, Chou M, Trapani AJ, Jeng AY (2000) Potent and selective non-peptidic inhibitors of endothelin-converting enzyme-1 with sustained duration of action. J Med Chem 43(3):488–504. https://doi.org/10.1021/jm990507o

Dhaun N, Webb DJ (2019) Endothelins in cardiovascular biology and therapeutics. Nat Rev Cardiol 16(8):491–502. https://doi.org/10.1038/s41569-019-0176-3

Doggrell SA (2004) Endothelin-converting enzyme inhibitors and their potential for cardiovascular and renal therapeutics. Expert Opin Ther Pat 14(5):655–665. https://doi.org/10.1517/13543776.14.5.655

Emoto N, Yanagisawa M (1995) Endothelin-converting enzyme-2 is a membrane-bound, phosphoramidon-sensitive metalloprotease with acidic pH optimum. J Biol Chem 270(25):15262–15268. https://doi.org/10.1074/jbc.270.25.15262

Fidan O, Yan R, Zhu D, Zhan J (2019) Improved production of antifungal angucycline Sch47554 by manipulating three regulatory genes in *Streptomyces* sp. SCC-2136. Biotechnol Appl Biochem 66(4):517–526. https://doi.org/10.1002/bab.1748

Hitzerd E, Neuman RI, Broekhuizen M, Simons SHP, Schoenmakers S, Reiss IKM, Koch BCP, Meiracker AHvd, Versmissen J, Visser W, Danser AHJ (2020) Transfer and vascular effect of endothelin receptor antagonists in the human placenta. Hypertension 75(3):877–884. https://doi.org/10.1161/hypertensionaha.119.14183

Ishikawa J, Hotta K (1999) FramePlot: a new implementation of the Frame analysis for predicting protein-coding regions in bacterial DNA with a high G+C content. FEMS Microbiol Lett 174(2):251–253. https://doi.org/10.1111/j.1574-6968.1999.tb13576.x

Jaeger RJR, Spiteller P (2010) Mycenaaurin A, an antibacterial polyene pigment from the fruiting bodies of *Mycena aurantiomarginata*. J Nat Prod 73(8):1350−1354. https://doi.org/10.1021/np100155z

Jiang D, Xin K, Yang B, Chen Y, Zhang Q, He H, Gao S (2020) Total synthesis of three families of natural antibiotics: anthrabenzoxocinones, fasamycins/naphthacemycins, and benastatins. CCS Chem 2:800–812. https://doi.org/10.31635/ccschem.020.202000151

Johnson GD, Stevenson T, Ahn K (1999) Hydrolysis of peptide hormones by endothelin-converting enzyme-1. A comparison with neprilysin. J Biol Chem 274(7):4053−4058. https://doi.org/10.1074/jbc.274.7.4053

Kaburagi S, Hasegawa K, Morimoto T, Araki M, Sawamura T, Masaki T, Sasayama S (1999) The role of endothelin-converting enzyme-1 in the development of α1-adrenergic-stimulated hypertrophy in cultured neonatal rat cardiac myocytes. Circulation 99(2):292−298. https://doi.org/10.1161/01.CIR.99.2.292

Kotha S, Cheekatla SR, Fatma A (2019) Syntheticapproach to the ABCD ring system of anticancer agent fredericamycin A via Claisen rearrangement and ring-closing metathesis as key steps. ACS Omega 4(17):17109−17116. https://doi.org/10.1021/acsomega.9b01178

Liu M, Jia Y, Xie Y, Zhang C, Ma J, Sun C, Ju J (2019) Identification of the actinomycin D biosynthetic pathway from marine-derived *Streptomyces costaricanus* SCSIO ZS0073. Mar Drugs 17(4):240. https://doi.org/10.3390/md17040240

Löffler BM (2000) Endothelin-converting enzyme inhibitors: current status and perspectives. J Cardiovasc Pharmacol 35(4 Suppl 2):S79−S82. https://doi.org/10.1097/00005344-200000002-00018

Lu F, Hou Y, Zhang H, Chu Y, Xia H, Tian Y (2017) Regulatory genes and their roles for improvement of antibiotic biosynthesis in *Streptomyces*. 3 Biotech 7(4):250. https://doi.org/10.1007/s13205-017-0875-6

Maglangit F, Fang Q, Leman V, Soldatou S, Ebel R, Kyeremeh K, Deng H (2019) Accramycin A, a new aromatic polyketide, from the soil bacterium, *Streptomyces* sp. MA37. Molecules 24(18):3384. https://doi.org/10.3390/molecules24183384

Martin P, Tzanidis A, Stein-Oakley A, Krum H (2000) Effect of a highly selective endothelin-converting enzyme inhibitor on cardiac remodeling in rats after myocardial infarction. J Cardiovasc Pharmacol 36(5, Suppl. 1):S367–S370. https://doi.org/10.1097/00005344-200036051-00106

Martínez-Miguel P, Raoch V, Zaragoza C, Valdivielso JM, Rodríguez-Puyol M, Rodríguez-Puyol D, López-Ongil S (2009) Endothelin-converting enzyme-1 increases in atherosclerotic mice: potential role of oxidized low density lipoproteins. J Lipid Res 50(3):364–375. https://doi.org/10.1194/jlr.M800215-JLR200

Martínez-Miguel P, Valdivielso JM, Medrano-Andrés D, Román-García P, Cano-Peñalver JL, Rodríguez-Puyol M, Rodríguez-Puyol D, López-Ongil S (2014) The active form of vitamin D, calcitriol, induces a complex dual upregulation of endothelin and nitric oxide in cultured endothelial cells. Am J Physiol Endocrinol Metab 307(12):E1085–E1096. https://doi.org/10.1152/ajpendo.00156.2014

Miyagawa K, Emoto N (2014) Current state of endothelin receptor antagonism in hypertension and pulmonary hypertension. Ther Adv Cardiovasc Dis 8(5):202–216. https://doi.org/10.1177/1753944714541511

Nakagawa Y, Doi T, Taketani T, Takegoshi K, Igarashi Y, Ito Y (2013) Mannose-binding geometry of pradimicin A. Chem Eur J 19(32):10516–10525. https://doi.org/10.1002/chem.201301368

Napan K, Zhang S, Morgan W, Anderson T, Takemoto JY, Zhan J (2014) Synergistic actions of tailoring enzymes in pradimicin biosynthesis. ChemBioChem 15(15):2289–2296. https://doi.org/10.1002/cbic.201402306

Newman DJ, Cragg GM (2020) Natural products as sources of new drugs over the nearly four decades from 01/1981 to 09/2019. J Nat Prod 83(3):770–803. https://doi.org/10.1021/acs.jnatprod.9b01285

Nolan M, Sikorski J, Jando M, Lucas S, Lapidus A, Glavina DRT, Chen F, Tice H, Pitluck S, Cheng J-F, Chertkov O, Sims D, Meincke L, Brettin T, Han C, Detter JC, Bruce D, Goodwin L, Land M, Hauser L, Chang Y-J, Jeffries CD, Ivanova N, Mavromatis K, Mikhailova N, Chen A, Palaniappan K, Chain P, Rohde M, Goker M, Bristow J, Eisen JA, Markowitz V, Hugenholtz P, Kyrpides NC, Klenk H-P (2010) Complete genome sequence of *Streptosporangium roseum* type strain (NI 9100). Stand Genomic Sci 2(1):29–37. https://doi.org/10.4056/sigs.631049

Overbeek R, Olson R, Pusch GD, Olsen GJ, Davis JJ, Disz T, Edwards RA, Gerdes S, Parrello B, Shukla M, Vonstein V, Wattam AR, Xia F, Stevens R (2013) The SEED and the Rapid Annotation of microbial genomes using Subsystems Technology (RAST). Nucleic Acids Res 42(D1):D206–D214. https://doi.org/10.1093/nar/gkt1226

Pavkov-Keller T, Steiner K, Faber M, Tengg M, Schwab H, Gruber-Khadjawi M, Gruber K (2017) Crystal structure and catalytic mechanism of CouO, a versatile C-methyltransferase from *Streptomyces rishiriensis*. PLOS ONE 12(2):e0171056. https://doi.org/10.1371/journal.pone.0171056

Qin Z, Devine R, Hutchings MI, Wilkinson B (2019) A role for antibiotic biosynthesis monooxygenase domain proteins in fidelity control during aromatic polyketide biosynthesis. Nat Commun 10(1):3611. https://doi.org/10.1038/s41467-019-11538-6

Ritzau M, Vettermann R, Fleck WF, Gutsche W, Dornberger K, Gräfe U (1997) Benaphthamycin, a new dihydrobenzo[α]naphthacenequinone antibiotic from *Streptomyces* sp. HKI-0057. J Antibiot 50(9):791–793. https://doi.org/10.7164/antibiotics.50.791

Rodríguez-Pascual F, Busnadiego O, Lagares D, Lamas S (2011) Role of endothelin in the cardiovascular system. Pharmacol Res 63(6):463–472 https://doi.org/10.1016/j.phrs.2011.01.014

Shao L, Zi J, Zeng J, Zhan J (2012) Identification of the herboxidiene biosynthetic gene cluster in *Streptomyces chromofuscus* ATCC 49982. Appl Environ Microbiol 78(6):2034–2038. https://doi.org/10.1128/AEM.06904-11

Smith TP, Haymond T, Smith SN, Sweitzer SM (2014) Evidence for the endothelin system as an emerging therapeutic target for the treatment of chronic pain. J Pain Res 7:531–545. https://doi.org/10.2147/JPR.S65923

Sun L, Zeng J, Cui P, Wang W, Yu D, Zhan J (2018) Manipulation of two regulatory genes for efficient production of chromomycins in *Streptomyces reseiscleroticus*. J Biol Eng 12:9/1-9/11. https://doi.org/10.1186/s13036-018-0103-x

Takahashi T, Kanda T, Inoue M, Sumino H, Kobayashi I, Iwamoto A, Nagai R (1998) Endothelin converting enzyme inhibitor protects against development of right ventricular overload and medial thickening of pulmonary arteries in rats with monocrotaline-induced pulmonary hypertension. Life Sci 63(10):PL137–PL143. https://doi.org/10.1016/S0024-3205(98)00347-6

Tian J, Chen H, Guo Z, Liu N, Li J, Huang Y, Xiang W, Chen Y (2016) Discovery of pentangular polyphenols hexaricins A–C from marine *Streptosporangium* sp. CGMCC 4.7309 by genome mining. Appl Microbiol Biotechnol 100(9):4189–4199. https://doi.org/10.1007/s00253-015-7248-z

Tsurumi Y, Fujie K, Nishikawa M, Kiyoto S, Okuhara M (1995) Biological and pharmacological properties of highly selective new endothelin converting enzyme inhibitor WS79089B isolated from *Streptosporangium roseum* No. 79089. J Antibiot 48(2):169–174. https://doi.org/10.7164/antibiotics.48.169

Tsurumi Y, Ohhata N, Iwamoto T, Shigematsu N, Sakamoto K, Nishikawa M, Kiyoto S, Okuhara M (1994) WS79089A, B and C, new endothelin converting enzyme inhibitors isolated from *Streptosporangium roseum* no. 79089: taxonomy, fermentation, isolation, physico-chemical properties and biological activities. J Antibiot 47(6):619–630. https://doi.org/10.7164/antibiotics.47.619

Wada A, Ohnishi M, Tsutamoto T, Fujii M, Matsumoto T, Yamamoto T, Wang X, Kinoshita M (2002) Chronic effects of an endothelin-converting enzyme inhibitor on cardiorenal and hormonal function in heart failure. Clin Sci 103(Suppl.):254S–257S. https://doi.org/10.1042/CS103S254S

Wada A, Tsutamoto T, Ohnishi M, Sawaki M, Fukai D, Maeda Y, Kinoshita M (1999) Effects of a specific endothelin-converting enzyme inhibitor on cardiac, renal, and neurohumoral functions in congestive heart failure: Comparison of effects with those of endothelin A receptor antagonism. Circulation 99(4):570–577. https://doi.org/10.1161/01.CIR.99.4.570

Whyteside AR, Turner AJ, Lambert DW (2014) Endothelin-converting enzyme-1 (ECE-1) is post-transcriptionally regulated by alternative polyadenylation. PloS one 9(1):e83260–e83260. https://doi.org/10.1371/journal.pone.0083260

Zhan J, Watanabe K, Tang Y (2008) Synergistic actions of a monooxygenase and cyclases in aromatic polyketide biosynthesis. ChemBioChem 9(11):1710–1715. https://doi.org/10.1002/cbic.200800178

Table 1 ^{1}H (300 MHz) and ^{13}C (75 MHz) NMR data for **5** in DMSO-d_6.

Position	δ_H	δ_C
1		170.5
2		107.5
3		162.1
3-OH	11.72 (1H, s)	
4		118.1
5		127.9
6		156.4
6-OH	13.78 (1H, s)	
7		115.2

8		188.0
9		125.0
10	7.93 (1H, d, 8.6)	125.9
11	7.28 (1H, d, 8.6)	121.3
12		159.0
12-OH	10.96 (1H, s)	
13		147.5
13-OCH_3	3.86 (3H, s)	61.3
14		129.4
15		182.4
16		122.8
17		149.9
17-OCH_3	3.93 (3H, s)	63.7
18		143.9
19	5.18 (1H, brs)	59.4
20	2.95 (1H, m)	38.2
	2.71 (1H, m)	
21		146.3
22	6.88 (1H, s)	119.7
23		140.9
24	3.05 (1H, m)	34.0
	2.92 (1H, m)	
25	4.88 (1H, m)	76.7
26	1.45 (3H, d, 6.2)	20.8

Table 2 Putative functions of the genes in the *wsa* gene cluster.

Gene	Size (aa)	Putative function	Homolog/GenBank accession no.	Identity/ similarity
wsaR1	263	TetR family transcriptional regulator	AcnR [*Streptomyces costaricanus*]/QAR15125	64/71
wsaO1	408	monooxygenase	FlsP [*Micromonospora rosaria*]/ALJ99865	52/65
wsaU1	102	Hypothetical protein	Hypothetical protein [*Streptosporangium minutum*]/WP_086575026	93/96
wsaO2	151	Monooxygenase	Hex33 [*Streptosporangium* sp. FXJ7.131]/AMK51290	99/99
wsaH5	285	Flavin-dependent oxidoreductase	Hex32 [*Streptosporangium* sp. FXJ7.131]/AMK51289	99/98
wsaW	126	Cyclase	Cyclase [*Streptomyces* sp. CNZ279]/WP_099879640	76/85
wsaV	245	Ketoreductase	Hex30 [*Streptosporangium* sp. FXJ7.131]/AMK51287	99/99
wsaO3	104	Monooxygenase	PdmH [*Actinomadura hibisca*]/ABM21754	58/73
wsaT	246	Ketoreductase	SimJ2 [*Streptomyces antibioticus*]/AAG34189	57/75
wsaS	562	NAD(P)/FAD-dependent oxidoreductase	Hex28 [*Streptosporangium* sp. FXJ7.131]/AMK51285	98/99

wsaQ	294	NAD(P)-dependent oxidoreductase	Hex27 [*Streptosporangium* sp. FXJ7.131]/AMK51284	98/98
wsaF	108	Cyclase	BenE [*Streptomyces* sp. A2991200]/CAM58796	62/76
wsaE	150	Cyclase	PdmL [*Actinomadura hibisca*]/ABK58685	60/73
wsaA	422	Ketosynthase	PdmA [*Actinomadura hibisca*]/ABM21747	77/86
wsaB	406	Chain length factor	PdmB [*Actinomadura hibisca*]/ABM21748	67/75
wsaC	86	Acyl carrier protein	PdmC [*Actinomadura hibisca*]/ABM21749	56/70
wasD	160	Aromatase	RubF [*Streptomyces collinus*]/AAG03070	72/79
wsaO4	157	Monooxygenase	Hex20 [*Streptosporangium* sp. FXJ7.131]/AMK51277	99/99
wsaG	243	Ketoreductase	PdmG [*Actinomadura hibisca*]/ABM21753.1	56/74
wsaH1	541	FAD-dependent oxidoreductase	TcmG [*Streptomyces lydicus*]/AJT61730	70/80
wsaR2	232	TenA family transcriptional regulator	Hex17 [*Streptosporangium* sp. FXJ7.131]/AMK51274	98/98
wsaU2	508	Hypothetical protein	Hex16 [*Streptosporangium* sp. FXJ7.131]/AMK51273	99/99
wsaI	446	Sodium:proton exchanger	DacR3 [*Dactylosporangium* sp. SC14051]/AFU65890	62/76
wsaU3	366	Hypothetical protein	Hex14 [*Streptosporangium* sp. FXJ7.131]/AMK51271	95/96
wsaJ	470	NAD(P)/FAD-dependent oxidoreductase or halogenase	Hex13 [*Streptosporangium* sp. FXJ7.131]/AMK51270	98/98
wsaH2	333	Flavin-dependent oxidoreductase	Hex12 [*Streptosporangium* sp. FXJ7.131]/AMK51269	98/98
wsaH3	285	Flavin-dependent oxidoreductase	Hex11 [*Streptosporangium* sp. FXJ7.131]/AMK51268	99/99
wsaO5	415	Monooxygenase	Hex10 [*Streptosporangium* sp. FXJ7.131]/AMK51267	98/99
wsaM1	337	Methyltransferase	TcmO [*Streptomyces lydicus*]/AJT61734	68/80
wsaK	281	NAD(P)H-binding protein	Hex8 [*Streptosporangium* sp. FXJ7.131]/AMK51265	99/99
wsaM2	344	Methyltransferase	Hex7 [*Streptosporangium* sp. FXJ7.131]/AMK51264	96/97
wsaL	64	Ferredoxin	Ferredoxin [*Actinomadura* sp. J1-007]/WP_164717208	76/88
wsaN	619	Asparagine synthetase	OxyD [*Streptomyces rimosus*]/AAZ78328	52/66
wsaP	199	Nitroreductase	Hex5 [*Streptosporangium* sp. FXJ7.131]/AMK51262	99/99
wsaH4	490	FAD-dependent oxidoreductase	Hex4 [*Streptosporangium* sp. FXJ7.131]/AMK51261	99/100
wsaO6	118	Monooxygenase	Hex3 [*Streptosporangium* sp. FXJ7.131]/AMK51260	96/96
wsaO7	104	Monooxygenase	GrhU [*Actinoplanes* sp. N902-109]/AGL16614	62/70
wsaR3	621	SARP family transcriptional regulator	Hex1 [*Streptosporangium* sp. FXJ7.131]/AMK51258	99/99

Figure legends

Fig. 1 Structures of **1**-**5** from *S. roseum* No. 79089.

Fig. 2 LC-MS analysis of the production of **1-5** by *S. roseum* No. 79089. **a** HPLC traces (460 nm) of the cultures of wild type (i) and *wsaA*-disrupted mutant (ii) strains of *S. roseum* No.

79089. **b** ESI-MS (-) spectrum of **1**. **c** ESI-MS (-) spectrum of **2**. **d** ESI-MS (-) spectrum of **3**. **e** ESI-MS (-) spectrum of **4**. **f** ESI-MS (-) spectrum of **5**.

Fig. 3 Key HMBC correlations for **5**.

Fig. 4 $\Delta\delta$ (δ_S-δ_R) values for the MTPA esters of **2**.

Fig. 5 The *wsa* biosynthetic gene cluster (**a**) and proposed biosynthetic pathways (**b**) of **1-5**.

Fig. 6 Gene disruption of *wsaA* in *S. roseum* No. 79089. **a** The strategy to disrupt *wsaA* in *S. roseum* No. 79089 through single crossover recombination. **b** PCR verification of the *wsa*A-disrupted mutant. M: 1 kb plus DNA ladder; 1: mutant; 2: wild type.

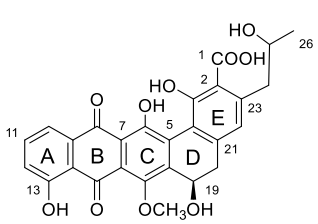

FR901533 or
WS79089B (**1**)

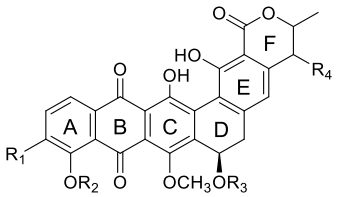

WS79089A (**2**) R_1=H, R_2=H, R_3=H, R_4=H
WS79089C (**3**) R_1=H, R_2=H, R_3=$COCH_3$, R_4=H
Benaphthamycin (**4**) R_1=H, R_2=H, R_3=H, R_4=OH
WS79089D (**5**) R_1=OH, R_2=CH_3, R_3=H, R_4=H

Fig. 1

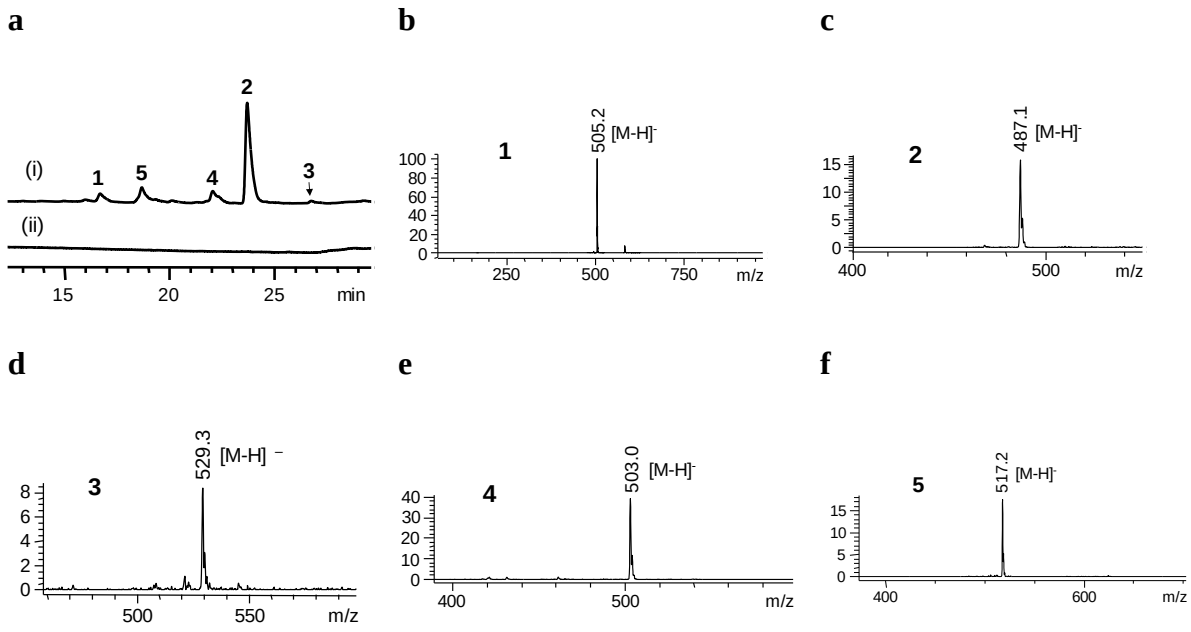

Fig. 2

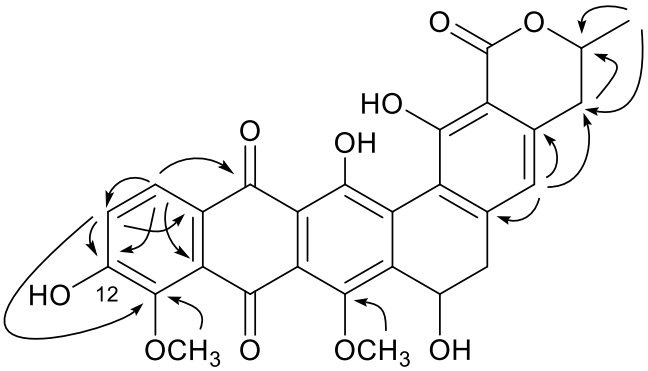

5

Fig. 3

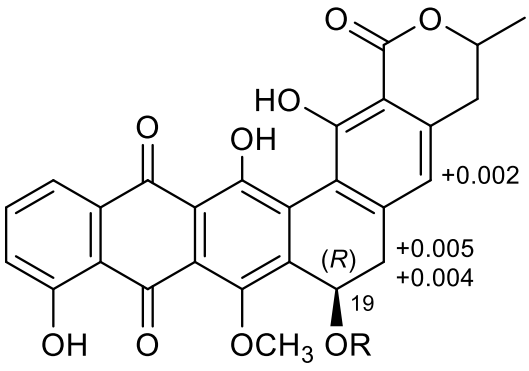

2S R = (*S*)-MPTA
2R R = (*R*)-MPTA

Fig. 4

a

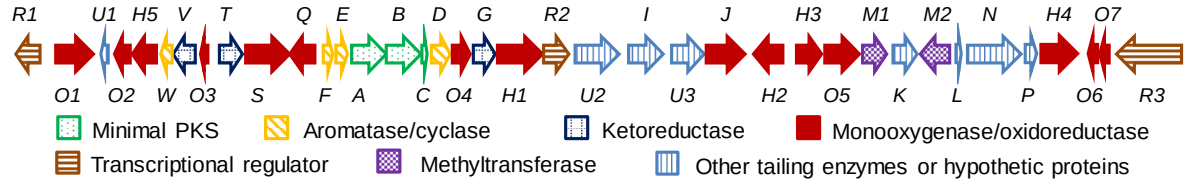
R1 U1 H5 V T Q E B D G R2 I J H3 M1 M2 N H4 O7
O1 O2 W O3 S F A C O4 H1 U2 U3 H2 O5 K L P O6 R3
Minimal PKS
Aromatase/cyclase
Ketoreductase
Monooxygenase/oxidoreductase
Transcriptional regulator
Methyltransferase
Other tailing enzymes or hypothetic proteins

b

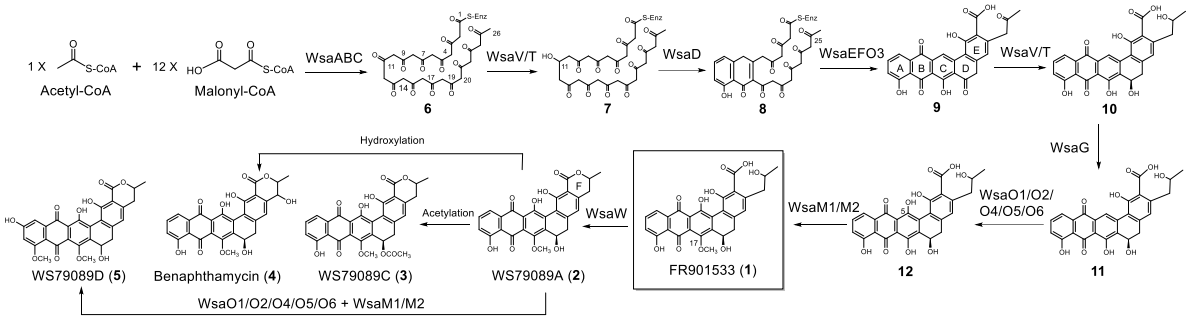
1 X
S-CoA
Acetyl-CoA
+ 12 X
HO
S-CoA
Malonyl-CoA
WsaABC
WsaV/T
WsaD
WsaEFO3
WsaV/T
6
7
8
9
10
WsaG
Hydroxylation
WS79089D (5)
Benaphthamycin (4)
WS79089C (3)
Acetylation
WS79089A (2)
WsaW
FR901533 (1)
WsaM1/M2
WsaO1/O2/
O4/O5/O6
12
11
WsaO1/O2/O4/O5/O6 + WsaM1/M2

Fig. 5

a

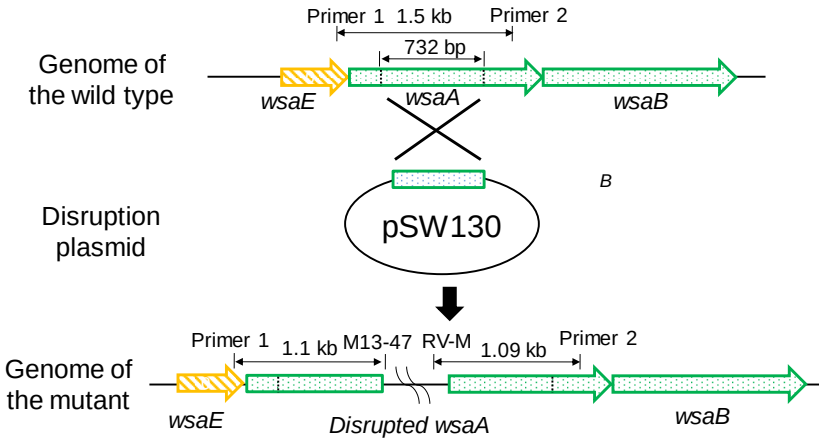
Primer 1
1.5 kb
Primer 2
732 bp
Genome of the wild type
wsaE
wsaA
wsaB
B
Disruption plasmid
pSW130
Primer 1
1.1 kb
M13-47
RV-M
1.09 kb
Primer 2
Genome of the mutant
wsaE
Disrupted wsaA
wsaB

b

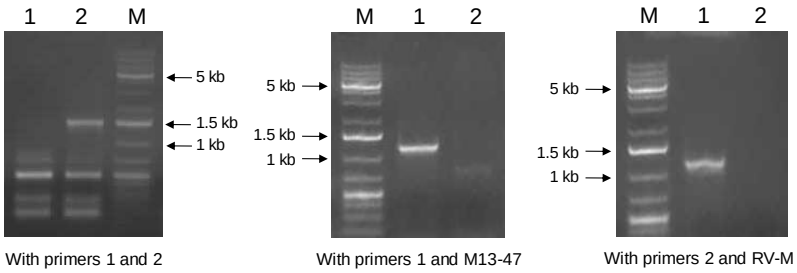
1
2
M
5 kb
1.5 kb
1 kb
With primers 1 and 2
M
1
2
5 kb
1.5 kb
1 kb
With primers 1 and M13-47
M
1
2
5 kb
1.5 kb
1 kb
With primers 2 and RV-M

Fig. 6